Journal of Applied Phycology (2021) 33:2561–2575
https://doi.org/10.1007/s10811-021-02469-1

The effects of four stressors, irradiance, temperature, desiccation, and salinity on the photosynthesis of a red alga, *Agarophyton vermiculophyllum* (Gracilariales) from a native distributional range in Japan

Ryo Kameyama[1] · Gregory N. Nishihara[2] · Chikara Kawagoe[3] · Ryuta Terada[4]

Received: 22 January 2021 / Revised and accepted: 12 April 2021 / Published online: 1 May 2021

Abstract

We examined the effects of four stressors, irradiance, temperature, desiccation, and salinity on the photosynthesis of a red alga, *Agarophyton vermiculophyllum* (= *Gracilaria vermiculophylla*, Gracilariales, Rhodophyta) from its native distributional range in Hokkaido and Kagoshima, Japan. Photosynthesis–irradiance (*P–E*) curves at 8, 16, and 28°C showed that the maximum net-photosynthetic rates (NP_{max}) and saturation irradiance (E_k) were highest at 28°C for both strains. Gross-photosynthesis determined at 8–40°C at 200 μmol photons m^{-2} s^{-1} showed that the maximum gross-photosynthetic rate (GP_{max}) occurred at 25.3°C for Hokkaido and 28.0°C for Kagoshima (T_{opt}^{GP}), which is almost consistent with the summer-time seawater temperature at each habitat. The temperature responses (4–40°C) of effective quantum yields ($\Delta F/F_m'$) of photosystem II during 7-day exposures were similar to that of oxygenic photosynthesis and the optimum temperature ($T_{opt}^{\Delta F/Fm'}$) was 20.0°C for Hokkaido and 30.1°C for Kagoshima. In the desiccation experiment, the $\Delta F/F_m'$ decreased with decreasing absolute water content (AWC); nevertheless, for samples with an AWC above 20%, $\Delta F/F_m'$ retuned to initial levels after subsequent 1-day rehydration in seawater, suggesting relatively strong tolerance to desiccation. This alga also showed a broad range of tolerance to salinity ranging from 20 to 60 psu in 7-day exposures, and the $\Delta F/F_m'$ tolerated 0 psu at 3-day exposure. The adaptations of *A. vermiculophyllum* from its native range in Japan to relatively high irradiance, a broad range of temperature, and strong osmotic (desiccation and salinity) tolerance explain its potentially high invasive capacity.

Keywords Algae · Desiccation stress · Rhodophyta · *Gracilaria vermiculophylla* · Invasive species · PAM fluorometry · Tolerance

Introduction

Invasive seaweeds are algal species that can successfully colonize areas outside range of their natural distribution (Williams and Smith 2007; Maggi et al. 2015). In general, the occurrence of invasive seaweeds in non-native regions may outcompete native algae and threaten the native ecosystem (Wallentinus and Nyberg 2007; Williams and Smith 2007; Maggi et al. 2015).

The red alga, *Agarophyton vermiculophyllum* (Ohmi) Gurgel, Norris et Fredericq (= *Gracilaria vermiculophylla* [Ohmi] Papenfuss; Gracilariales; Terada and Yamamoto 2002; Gurgel et al. 2018) was originally described from Akkeshi, Hokkaido, Japan by Ohmi in 1956 (as *Gracilariopsis vermiculophylla* Ohmi; Ohmi 1956, 1958; Terada and Yamamoto 2002) and is known to be native to temperate and subarctic coasts of East Asia, especially Japan,

✉ Ryuta Terada
terada@fish.kagoshima-u.ac.jp

[1] Faculty of Fisheries, Kagoshima University, Shimoarata 4-50-20, Kagoshima City, Kagoshima 890-0056, Japan

[2] Institute for East China Sea Research, Graduate School of Fisheries and Environmental Sciences, Organization for Marine Science and Technology, Nagasaki University, Taira-machi 1551-7, Nagasaki City, Nagasaki 851-2213, Japan

[3] Algatech-Kyowa Technical Laboratory of Seaweeds, Kyowa Concrete Industry Co. Ltd., Bentencho 24-13, Hakodate City, Hokkaido 040-0051, Japan

[4] United Graduate School of Agricultural Sciences, Kagoshima University, Korimoto 1-21-24, Kagoshima City, Kagoshima 890-0065, Japan

China, Korea, and Russia (Yamamoto 1978; Tseng and Xia 1999; Terada and Yamamoto 2002; Boo and Ko 2012; Titlyanov and Titlyanova 2012). This species is regarded as an edible agarophyte in Japan (Ohmi 1958; Ohno and Largo 1998); nevertheless, it is also known to be a highly invasive species outside of the northwestern Pacific. In fact, this alga has been introduced to the northeastern Pacific and northern Atlantic waters in the past a few decades; the shipping and import of Japanese oysters to these regions are believed to be one vector of its introduction (Bellorin et al. 2004; Rueness 2005; Thomsen et al. 2006, 2007, 2009; Freshwater et al. 2006a, b; Saunders 2009; Kim et al. 2010). According to oyster aquaculture records and generic data reported in recent articles, it is believed that there were at least three primary invasions into each of the three continental margins in the northern hemisphere, followed by a secondary spread along each coastline (Barrett 1963; Ruesink et al. 2005; Krueger-Hadfield et al. 2016).

Introduced populations of *A. vermiculophyllum* have been reported to outcompete native macroalgae and seagrasses and dominate ecosystems (Martínez-Lüscher and Holmer 2010; Hammann et al. 2013a). Based on these concerns to the coastal ecosystem, studies on the ecology, physiology, and population genetics for this alga elucidates their ability to adapt and tolerate a variety of environment conditions and attempts to identify the origin and vectors of introduction (e.g., Yokoya et al. 1999; Raikar et al. 2001; Rueness 2005; Weinberger et al. 2008; Byers et al. 2012; Nejrup and Pedersen 2012; Nejrup et al. 2013; Hammann et al. 2013a, b; Krueger-Hadfield et al. 2016, 2017; Gorman et al. 2017; Sotka et al. 2018). For instance, the ecological success of this alga in introduced habitats is considered to be attributed to its high stress tolerance, resistance to herbivory, and in some areas, an absence of other macroalgal competitors (Yokoya et al. 1999; Raikar et al. 2001; Byers et al. 2012; Nejrup and Pedersen 2012; Hammann et al. 2013a, b).

Recent studies suggest that the characteristics of growth and tolerance to environmental gradients between the individuals from native and introduced regions are likely different; perhaps rapid phenotypic evolution has been occurring during invasion that enables the adaptation to non-native regions (Krueger-Hadfield et al. 2016, 2017; Gorman et al. 2017; Sotka et al. 2018). Studies of *A. vermiculophyllum* from its native range have been restricted to growth experiments and genetic and phylogeographical studies (Yokoya et al. 1999; Raikar et al. 2001; Krueger-Hadfield et al. 2016, 2017; Gorman et al. 2017; Sotka et al. 2018). Information regarding photosynthesis of this alga from its native range under an environmental gradient is limited, with the exception of an examination of oxygen production (Phooprong et al. 2008). Additional insight regarding its photobiology, in relation to adaptation to an environmental gradient, is expected to lead to a more in depth understanding of adaptation within its native range. Furthermore, such insight is expected to enhance understanding of where and how *A. vermiculophyllum* can successfully invade new ecosystems.

In the present study we examine the hypothesis that *A. vermiculophyllum* can photosynthesize under a wide environmental stress gradient, and focused on elucidating the photosynthetic response of this alga from its native distributional range in Japan along an environmental stress gradient of irradiance, temperature, desiccation, and salinity, using a pulse amplitude modulation (PAM)-chlorophyll fluorometer and optical dissolved oxygen sensors.

Materials and methods

Sample collection and stock maintenance

Agarophyton vermiculophyllum is divided into two haplotypes that are distributed separately in northern and southern Japan; those of northern Japan are regarded to be identical with the taxon occurring in introduced areas (Krueger-Hadfield et al. 2017). In the present study, we used samples of both haplotypes for the experiment (more than 100 individuals for each collection date/site). Those from northern strain (Hokkaido; see Krueger-Hadfield et al. 2017) were collected from intertidal rocks and pebbles at Shinori, Hakodate City (41° 46' N 140° 49' E), Hokkaido on 4 July 2016, 8 July 2017, and 22 June 2020. Those from the southern strain (Kagoshima) were collected from intertidal rocks and pebbles at Terushima, Ichiki-Kushikino City (31° 42' N, 130° 16' E), Kagoshima on 15 December 2016, 10 June 2017, and 22 June 2020. Samples were transported to the laboratory of Marine Botany, Kagoshima University in coolers at around 20°C, which was the seawater temperature during the sampling periods. Samples were maintained before examination in two aquarium tanks (200 L each) at 33 psu, pH of 8.0–8.1, 20°C, and irradiance of ca. 80 μmol photons m^{-2} s^{-1} (14:10 h light: dark cycle). Algal stocks were continuously maintained until the experiments were completed within a few weeks in every year.

Effect of irradiance on the oxygenic photosynthesis at 8, 16, and 28°C

The samples used in the experiments were collected in 2016 (for 16°C) and 2017 (for 8 and 28°C). The oxygenic net photosynthetic rates were determined at 0, 30, 60, 100, 150, 200, 250, 500, and 1000 μmol photons m^{-2} s^{-1} ($n = 5$ per irradiance level), at 8, 16 and 28°C, respectively. These three temperature treatments were assigned based on the early-winter seawater temperature at Hokkaido (8°C; December–January; Terada et al. 2000, 2021), those at Kagoshima (16°C,

December–January; Watanabe et al. 2014; Terada et al. 2021), and the highest seawater temperature at Kagoshima (28°C, Watanabe et al. 2014; Terada et al. 2021).

Dissolved oxygen (DO) was measured using DO meters equipped with optical dissolved oxygen sensors (ProODO-BOD, YSI Incorporated, USA). A metal-halide lamp was used as light source (MHN-150D-S, Nichido Ind. Co. Ltd, Japan), and a spherical (4π) submersible quantum sensor (LI-192, LI-250A, LI-COR, USA) was used to set the irradiance.

Methods for these photosynthesis–irradiance (*P–E*) experiments are described in detail in our past studies (e.g., Terada et al. 2020a). Briefly, explants (branch and branchlet of alga; ca. 300 mg for each replication) were pre-incubated overnight (ca. 12 h) with sterilized natural seawater in an incubator at each experimental temperature treatment. On the day of the experiment, explants were randomly selected and placed in 100 mL BOD bottles (YSI Japan's genuine product) containing sterilized natural seawater. The DO sensors were then set carefully into the BOD bottles so that no bubbles were trapped. DO concentrations (mg L^{-1}) were measured every 5 min for 30 min after a 30-min pre-acclimation to each experimental irradiance. Seawater was continuously stirred throughout the measurement, with the experimental temperatures maintained using a water bath with a circuit chiller. The exact volumes of the BOD bottles were determined after the experiments and were used to estimate photosynthesis and dark respiration rates. Seawater medium was renewed after each irradiance exposure and measurement to avoid any effects that can be attributed to nutrient and dissolved carbon dioxide depletion. *P–E* experiments started at 0 μmol photons m^{-2} s^{-1} and finished at 1000 μmol photons m^{-2} s^{-1}. Dark respiration and net photosynthetic rates were estimated by fitting a first-order linear model to the collected data.

Effect of temperature on the oxygenic photosynthesis and dark respiration

The samples used in the experiments were collected in 2016 (Hokkaido strain) and 2017 (Kagoshima strain). Measurements (ca. 300 mg for each replication) were conducted at nine temperature levels (8, 12, 16, 20, 24, 28, 32, 36, and 40°C; $n = 5$ per temperature level) under an irradiance of 200 μmol photons m^{-2} s^{-1} (based on the saturation irradiance of the *P–E* curve at 16°C). The temperatures were adjusted with a water bath by using the circuit chiller that was mentioned above. DO concentrations were measured every five-minutes over a 30-min interval, with 30 min of pre-acclimation to each temperature. Respiration rates were measured after 10 min of dark acclimation by wrapping the BOD bottles with aluminum foil.

Temperature effect on the photochemical efficiency of photosystem II (PSII)

The samples used in the experiments were collected in 2020, and Mini Imaging-PAM (Heinz Walz GmbH, Germany) measurements were modified from the procedure in our previous studies (e.g., Terada et al. 2020a, 2020b). The branch and branchlet of algae (ca. 5 cm-long) were cut and pre-incubated overnight in the dark at 20°C. To start the experiment, samples (10 individuals per temperature level) were then placed in 500-mL flasks and were incubated under the irradiance of 50 μmol photons m^{-2} s^{-1} (14L10D photoperiod) at ten temperatures (4, 8, 12, 16, 20, 24, 28, 32, 36, and 40°C) for 7 days (Eyela MTI-201B, Tokyo Rikakikai Co., Ltd., Japan). The effective quantum yields of PSII ($\Delta F/F_m' = \Phi_{PSII}$) at each temperature was measured at 1-, 3-, and 7-day temperature exposure ($n = 10$ per temperature). At the measurement of $\Delta F/F_m'$, samples were haphazardly selected and placed in a stainless-steel tray (12×10×3 cm) containing sterilized natural seawater. Seawater temperature in the tray was controlled with an aluminum block incubator (BI-536T, Astec, Japan), and monitored with a thermocouple (testo 925, Testo AG, Germany).

The chronic effect of desiccation on the photochemical efficiency and the potential of recovery after rehydrated in seawater

The samples used in the experiments were collected in 2020, and the method of this experiment was modified from the procedure in our recent study (Terada et al. 2020b). One day before the experiment, the samples were pre-incubated overnight (12 h) in the dark at 20°C. Before starting the experiment, the $\Delta F/F_m'$ from the samples randomly selected ($n = 10$ per individual; five individuals at each desiccation period; therefore, total number of the measurements at each desiccation period is 50, $n = 50$ per period) was measured in seawater at 20°C under the dim-light (20 μmol photons m^{-2} s^{-1}) to provide initial values. The reason why ten different portions were measured from one individual was that the proceed of desiccation was not a uniform in the thallus (i.e., marginal and central portions). Samples were placed on the Petri dish after gently removing the seawater from the surface by using Kimwipes prior to measurement. The aerial exposure was conducted up to 480 min (0, 5, 10, 30, 60, 120, 240, and 480 min treatments, respectively) under the ca. 50% humidity with the dim-light (20 μmol photons m^{-2} s^{-1}) at 20°C.

To elucidate the status of $\Delta F/F_m'$ and the potential of recovery after subsequent rehydration in seawater at each aerial exposure period, $\Delta F/F_m'$ ($n = 50$ per period) was determined at three different conditions (while the samples exposed in air, 30-min and 1-day after subsequent rehydration in seawater) at every treatment of 5, 10, 30, 60, 120, 240, and 480 min of

continuous aerial exposure. Specifically, the samples were picked up from the petri dish at each period of desiccation, and the $\Delta F/F_m'$ was measured immediately at desiccation state. Thereafter, the samples were rehydrated in seawater. At 30-min and 24-h after subsequent rehydration in seawater, the $\Delta F/F_m'$ was also determined to confirm the potential of recovery. Humidity was monitored during the experiment by a hygrometer (testo 610, Testo AG, Germany).

To elucidate the relationship between the $\Delta F/F_m'$ and water loss from the thallus, we also monitored the initial wet weight, wet weight after each desiccation period, and dry weight of the samples. The wet weight of the samples was measured by an electric balance (AB54-S, Mettler Toledo LLC, USA) after removing the seawater on the surface by using Kimwipes. The thallus was dried for 48 h at 60°C for dry weight measurements. The absolute water content (AWC) was determined using Eq. 1 (Wang et al. 2011; Gao and Wang 2012; Gao et al. 2013; Watanabe et al. 2017):

$$\text{Absolute Water Content}\,(AWC,\%) = \frac{(W_t - W_d)}{(W_0 - W_d)} \times 100 \quad (1)$$

where W_d is the dry weight (the weight of blades after drying for 48 h at 60°C), W_0 is the wet weight (the weight of the fresh blades after the gentle removal of water from the surface), and W_t is the weight at time t after dehydration. The number of $\Delta F/F_m'$ replications per each individual was ten (n = 10).

The chronic effect of salinity on the photochemical efficiency

The samples used in the experiments were collected in 2020. One day before the experiment, the samples of the branches and branchlets of algae (ca. 5-cm long) were acclimated overnight (12 h) in the dark at 20°C. Before starting the experiment, the $\Delta F/F_m'$ from the samples randomly selected was measured in seawater under the dim-light (20 μmol photons m^{-2} s^{-1}) to confirm the initial status. Samples (10 individuals per level) were then placed in 500 mL flasks at eight salinity levels (0, 10, 20, 30, 34, 40, 50, and 60 psu) for 7 days at 20°C under the dim-light (14L10D). The salinity at 34 psu was similar to the seawater at the collection sites. The measurement of $\Delta F/F_m'$ (n = 10 per level) was done at 3-day and 7-day culture. The salinity was adjusted by the freshwater and sodium chloride. However, dilution by freshwater causes the dilution of nutrients; therefore, we added Provasoli's enriched seawater (PES) medium for all treatments to ensure no different effect from the nutrients by levels.

Modeling the photosynthetic response to temperature and irradiance

For each strain (Hokkaido and Kagoshima), a Bayesian approach was used to analyze the response of photosynthesis to the temperature and irradiance gradients. The model to describe the response of the effective quantum yields to temperature was a thermodynamic non-linear model that hypothesizes that physiological rates enters a less active state above an optimal temperature (Eq. 2; Thornley and Johnson 2000; Alexandrov and Yamagata 2007).

$$y = \frac{y_{max} H_d \exp\left(\frac{H_a}{R}\left(\frac{1}{K_{opt}} - \frac{1}{K}\right)\right)}{H_d - H_a\left(1 - \exp\left(\frac{H_d}{R}\left(\frac{1}{K_{opt}} - \frac{1}{K}\right)\right)\right)} \quad (2)$$

In this equation, y is the response variable, which is the effective quantum yield ($\Delta F/F_m'$). The temperature scale is Kelvin (K). The model has four parameters: y_{max} scales the model to the range of y. K_{opt} is the absolute temperature where y is maximized, H_a is the activation energy in kJ mol^{-1} and H_d is the deactivation energy in kJ mol^{-1}. R in this model is the ideal gas constant and has a value of 8.314 J mol^{-1}.

Given the large number of zeros in the measurements, a zero-inflated beta distribution (Borlongan et al. 2020) was used and the zero-inflation rate was modeled as a temperature linear regression. The link-function for the data was the identity function, a log function was the link-function for the shape parameter (Φ) of the beta distribution, a logit function was the link-function for the zero-inflation rate.

The gross photosynthesis rate (GP), which is assumed as a hidden state, was estimated by simultaneously fitting the measured dark respiration rates (R_d) to the Arrhenius equation (Eq. 3), and the observed net photosynthesis rates (NP) to the difference in Eqs. 2 and 3. Under light conditions, both photorespiration and non-photorespiratory (i.e., mitochondrial) reactions result in oxygen consumption (Tcherkez et al. 2008); however, it is not uncommon for the differences between respiration rates under light and dark conditions to be insignificant (Bellasio et al. 2014). Hence, photorespiration was assumed to be adequately described by the dark respiration rate. R_m is the respiration rate at the arbitrary reference temperature (i.e., mean temperature of 24°C; K_m = 295.15) and E_a is the activation energy.

$$R_d = R_m exp\left(-\frac{E_a}{R}\left(\frac{1}{K} - \frac{1}{K_m}\right)\right) \quad (3)$$

The response of photosynthesis to irradiance was examined by modeling the data using an exponential equation (Jassby and Platt 1976; Webb et al. 1974; Platt et al. 1980; Henley

1993) which had the form:

$$P_{net} = P_{max}\left(1-exp\left(\frac{-\alpha}{P_{max}}E\right)\right)-R_d \quad (4)$$

where P_{net} is the net O_2 production rate, P_{max} is the maximum O_2 production rate, α is the initial slope of the *P–E* curve, E is the incident irradiance, and R_d is the dark respiration rate. From this model, the saturation irradiance (E_k) was calculated as P_{max} / α and the compensation irradiance (E_c) was $P_{max} ln\left(\frac{P_{max}}{(P_{max}-R_d)}\right)/\alpha$.

Statistical analysis

Statistical analyses of all the models were conducted using R version 4.0.3 (R Core Team 2020), and model fitting was done using the package brms version 2.14.0 (Bürkner 2018). The parameters were determined by fitting the relevant models using Bayesian methods. The package brms using RStan (Stan Development Team 2020) as the backend to sample from the posterior distributions of the parameters, and four chains of at least 6000 samples per chain were generated and assessed for convergence. Typically, at least 1000 samples of the parameters of interest are generated. Informative normal priors were placed on all parameters of the model by using values from a previous study (Kokubu et al. 2015), and a half-Cauchy prior distribution was placed on the scale parameter of the models (Gelman 2004, 2006). The error distribution for the gross photosynthetic rate analysis was the gaussian distribution, and a beta distribution was used for the analysis of the effective quantum yield.

Differences in the $\Delta F/F_m'$ of the alga in the desiccation-rehydration experiments over time were analyzed with one-factor ANOVA and with the fixed factor "desiccation treatment" (at four levels: initial $\Delta F/F_m'$, $\Delta F/F_m'$ after desiccation treatment, and $\Delta F/F_m'$ after 30-min and1-d rehydration in seawater). Those in salinity response were also analyzed with one-factor ANOVA and with the fixed factor "salinity treatment" (initial level at 34 psu, after salinity treatment at each level).

Results

Effect of irradiance on the oxygenic photosynthesis at 8, 16, and 28°C

The oxygenic net photosynthetic (P_{net}) rates of the Hokkaido and Kagoshima strains determined at 8, 16, and 28°C, steadily increased with increasing irradiance, and then approached saturation (Fig. 1). Based on the model fitted *P–E* curve in the Hokkaido strain, the maximum net photosynthetic rates (NP_{max}) at 8, 16, and 28°C were estimated to be 5.68 (5.22–6.19, 95% highest density credible intervals, 95% HDCI), 20.53 (19.52–21.54, 95% HDCI) and 27.93 (25.79–30.42, 95% HDCI) μg O_2 g_{ww}^{-1} min^{-1}, respectively (Fig. 1, Table 1). Likewise, saturation irradiance (E_k) also increased with rise in temperature treatment and was 74 (55–95, 95% HDCI), 184 (164–207, 95% HDCI), and 423 (350–514, 95% HDCI) μmol photons m^{-2} s^{-1} at 8, 16, and 28°C, respectively. Other parameters estimate including the initial slope (α) and dark respiration (R_d) rates, and compensation irradiance (E_c) are shown in Table 1.

Regarding the model fitted *P–E* curve in the Kagoshima strain, the maximum net photosynthetic rates (NP_{max}) at 8, 16, and 28°C were estimated to be 2.86 (2.56–3.25, 95% HDCI), 43.31 (40.90–45.78, 95% HDCI), and 48.39 (45.01–52.30 95% HDCI) μg O_2 g_{ww}^{-1} min^{-1}, respectively (Fig. 1, Table 2). Saturation irradiance (E_k) was suppressed at 8°C as 7 (1–21, 95% HDCI) μmol photons m^{-2} s^{-1}; however, it also increased with rise in temperature treatment and was 234 (205–267, 95% HDCI), and 499 422–589, 95% HDCI) μmol photons m^{-2} s^{-1} at 16 and 28°C. Other parameters estimate including the initial slope (α) and dark respiration (R_d) rates, and compensation irradiance (E_c) are shown in Table 2.

Effect of temperature on the oxygenic photosynthesis and dark respiration

Measured *NP* rates of the Hokkaido and Kagoshima strains at 200 μmol photons m^{-2} s^{-1} showed a dome-shaped temperature response (Fig. 2). Dark respiration of the Hokkaido and Kagoshima strains was likewise temperature dependent, with rates gradually increasing from 0.59 (± 0.42 standard deviation, SD) and 0.29 (± 0.50) μg O_2 g_{ww}^{-1} min^{-1} at 8°C to 3.61 (± 0.73) and 3.84 (± 0.92) μg O_2 g_{ww}^{-1} min^{-1} at 40°C, respectively (Fig. 2). On the gross photosynthesis–temperature ($GP-T$) model derived from the P_{net}–temperature response and the dark respiration, those of the Hokkaido strain showed the dome-shaped and indicated that the maximum gross photosynthetic rate (GP_{max}) was 13.09 μg O_2 g_{ww}^{-1} min^{-1} (12.06–14.10, 95% HDCI) and occurred at 25.3°C (23.2–27.6, 95% HDCI) as the optimal temperature (T_{opt}^{GP}, Table 3). In contrast, GP_{max} of Kagoshima was 26.56 μg O_2 g_{ww}^{-1} min^{-1} (24.96–28.19, 95% HDCI) at the T_{opt}^{GP} of 28.0°C (26.0–29.9, 95% HDCI). Other model parameter estimates are presented in Table 3.

Temperature effect on the photochemical efficiency of PSII

In general, the temperature exposure experiments revealed that the effective quantum yields of PSII ($\Delta F/F_m'$) of the Hokkaido and Kagoshima strains were dome-shaped in

Table 1 Mean and 95% highest density credible intervals (95% HDCI) of *P–E* parameters of a red alga, *Agarophyton vermiculophyllum* from Hokkaido, Japan, at 8, 16, and 28°C. NP_{max} = maximum net photosynthesis (μg O_2 g_{ww}^{-1} min^{-1}); α = initial slope [μg O_2 g_{ww}^{-1} min^{-1} (μmol photons m^{-2} s^{-1}) $^{-1}$]; R_d = respiration rate (μg O_2 g_{ww}^{-1} min^{-1}); E_c = compensation irradiance (μmol photons m^{-2} s^{-1}); E_k = saturation irradiance (μmol photons m^{-2} s^{-1})

	8 °C		16 °C		28 °C	
Parameter	Mean	95% HDCI	Mean	95% HDCI	Mean	95% HDCI
NP_{max}	5.68	5.22–6.19	20.53	19.52–21.54	27.93	25.79–30.42
α	0.08	0.06–0.10	0.11	0.10–0.13	0.07	0.06–0.08
R_d	0.15	0.00–0.52	1.99	1.25–2.76	1.81	0.91–2.73
E_c	2	0–6	19	13–24	28	16–39
E_k	74	55–95	184	164–207	423	350–514

response to temperature (Fig. 3). Notably, $\Delta F/F_m'$ dropped to zero at the 7-day exposure treatment when temperature was 40°C for both strains.

The mean and standard deviations of the measured $\Delta F/F_m'$ of the Hokkaido strain after 1-day was 0.414 ± 0.021 SD at 4°C and reached a high of 0.468 ± 0.012 at 24°C before declining to 0.141 ± 0.060 at 40°C. After the 3-day treatment, the measured $\Delta F/F_m'$ was 0.368 ± 0.020 at 4°C and reached a high of 0.482 ± 0.022 at 20°C before declining to zero by 40°C. Similarly, after the 7-day treatment, the measured $\Delta F/F_m'$ was 0.382 ± 0.033 at 4°C and reached a high of 0.490 ± 0.020 at 20°C before declining to zero by 36°C.

The mean and standard deviations of the measured $\Delta F/F_m'$ of the Kagoshima strain all peaked at 20°C and did not decline to zero at 40°C. After the 1-day treatment the $\Delta F/F_m'$ was 0.362 ± 0.031 SD at 4°C and reached a high of 0.464 ± 0.019 at 20°C before declining to 0.356 ± 0.034 at 40°C. After the 3-day treatment, the measured $\Delta F/F_m'$ was 0.357 ± 0.028 at 4°C and reached a high of 0.461 ± 0.037 at 20°C before declining to 0.328 ± 0.044 at 40°C. Similarly, after the 7-day treatment, the measured $\Delta F/F_m'$ was 0.294 ± 0.045 at 4°C and reached a high of 0.483 ± 0.017 at 20°C before declining to 0.037 ± 0.055 at 40°C.

Based on the model and data, the 1-, 3-, and 7-day exposure treatment parameters of Fig. 3 are provided in Tables 4 and 5.

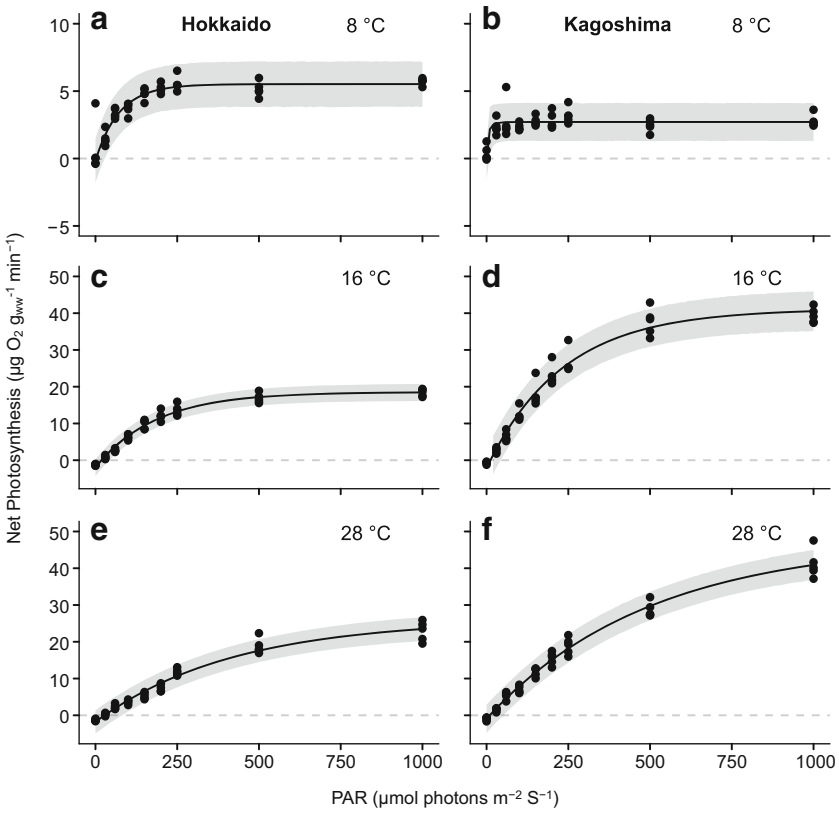

Fig. 1 The response of the net photosynthetic rates of a red alga, *Agarophyton vermiculophyllum* from the native range of distribution in Hokkaido (A, C, E) and Kagoshima (B, D, F), Japan to irradiance at 8°C (A, B), 16°C (C, D), and 28°C (E, F). The dots indicate the actual measured rates (n = 5 at level), the lines indicate the expected value, and the shaded regions indicate the 95% highest density credible interval (95% HDCI) of the model

Table 2 Mean and 95% highest density credible intervals (95% HDCI) of *P–E* parameters of a red alga, *Agarophyton vermiculophyllum* from Kagoshima, Japan, at 8, 16, and 28°C. NP_{max} = maximum net photosynthesis (μg O_2 g_{ww}^{-1} min^{-1}); α = initial slope [μg O_2 g_{ww}^{-1} min^{-1} (μmol photons m^{-2} s^{-1}) $^{-1}$]; R_d = respiration rate (μg O_2 g_{ww}^{-1} min^{-1}); E_c = compensation irradiance (μmol photons m^{-2} s^{-1}); E_k = saturation irradiance (μmol photons m^{-2} s^{-1})

	8 °C		16 °C		28 °C	
Parameter	Mean	95% HDCI	Mean	95% HDCI	Mean	95% HDCI
NP_{max}	2.86	2.56–3.25	43.31	40.90–45.78	48.39	45.01–52.30
α	0.81	0.14–2.31	0.19	0.16–0.21	0.10	0.09–0.11
R_d	0.15	0.00–0.49	2.15	0.59–3.77	0.93	0.09–2.00
E_c	0	0–2	12	4–19	10	1–19
E_k	7	1–21	234	205–267	499	422–589

Briefly, in the Hokkaido strain, the optimal temperature ($T_{opt}^{\Delta F/Fm'}$) was highest for the 1-day experiment (26.1°C; 24.2–28.0, 95% HDCI) and declined to 20.0°C (18.5–21.5, 95% HDCI) by day 7. The maximum $\Delta F/F_m'$ ($\Delta F/F_m'$ max) after 1-, 3-, and 7-day exposure was estimated to be 0.45 (0.44–0.46, 95% HDCI), 0.49 (0.47–0.50, 95% HDCI), and 0.50 (0.48–0.51, 95% HDCI), respectively. In contrast, for the Kagoshima strain, the $T_{opt}^{\Delta F/Fm'}$ increased from 16.5°C (14.1–18.9, 95% HDCI) at day 1 to 30.1°C (27.9–32.2, 95% HDCI) at day 7. The $\Delta F/F_m'$ max after 1-, 3-, and 7-day exposure was estimated to be 0.47 (0.46–0.48, 95% HDCI), 0.46 (0.45–0.48, 95% HDCI), and 0.46 (0.43–0.48, 95% HDCI), respectively. Other model parameter estimates are presented in Tables 4 and 5.

The chronic effect of desiccation on the photochemical efficiency and the potential of recovery after rehydrated in seawater

In the Hokkaido strain, $\Delta F/F_m'$ of the alga under aerial exposure was stable from the initial value (0.446 ± 0.018 SD) to those until 30-min exposure (0.449 ± 0.030 at 10-min, 100.6% from the initial value; 0.440 ± 0.023 at 30-min, 98.6%; Fig. 4 A). Nevertheless, $\Delta F/F_m'$ decreased with increasing desiccation period at 1-, 2-, and 4-h exposures (0.342 ± 0.083 at 1-h, 76.5%; 0.179 ± 0.131 at 2-h, 40.1%; and 0.013 ± 0.047 at 4-h, 2.9%; $P < 0.001$) and zero at 8-h exposure, respectively. After subsequent 30-min rehydration in seawater, the $\Delta F/F_m'$ of alga at desiccation treatments of 1-h exposure likewise returned to the initial level (0.470 ± 0.030 at 10-min, 98.5%; 0.482 ± 0.030 at 30-min, 101.1%; 0.462 ± 0.042 at 1-h, 96.7%); however, those at 2-, 4-, and 8-h exposure treatments failed to recover (0.384 ± 0.106 at 2-h, 80.5%; 0.121 ± 0.150 at 4-h, 25.4%; 0.002 ± 0.006 at 8-h, 0.39%; $P < 0.001$; Fig. 4C). Furthermore, after 1-day rehydration in seawater, those at 2-h desiccation treatments also returned to the initial level (0.464 ± 0.043, 102.2%). Nevertheless, those at 4-, and 8-h exposure failed to recover even after 1-day rehydration in seawater (0.200 ± 0.172 at 4-h, 44.2%; 0.012 ± 0.012 at 8-h, 2.7%; $P < 0.001$; Fig. 4E).

The, $\Delta F/F_m'$ of the alga from Kagoshima was generally stable from its initial value (0.481 ± 0.036 SD) to that at 10-min exposure (0.469 ± 0.055; 97.4%); however, the $\Delta F/F_m'$ decreased with increasing desiccation period at 30-min, 1-h, and 2-h exposures (0.389 ± 0.080 at 30-min, 80.9% from the

Table 3 Mean and 95% highest density credible intervals (95% HDCI) of the parameters estimated for the gross photosynthesis–temperature model in a red alga, *Agarophyton vermiculophyllum* from Hokkaido and Kagoshima, Japan. GP_{max} = maximum gross photosynthesis (μg O_2 g_{ww}^{-1} min^{-1}); H_a = activation energy for photosynthesis (kJ mol^{-1}); H_d = deactivation energy (kJ mol^{-1}); T_{opt}^{GP} = optimum temperature (°C); E_a = activation energy for respiration (kJ mol^{-1})

	Hokkaido		Kagoshima	
Parameter	Mean	95% HDCI	Mean	95% HDCI
GP_{max}	13.09	12.05–14.10	26.56	24.96–28.19
H_a	29	19–42	26	18–36
H_d	166	121–231	200	142–275
T_{opt}^{GP}	25.3	23.2–27.6	28.0	26.0–29.9
E_a	47	35–60	59	47–71

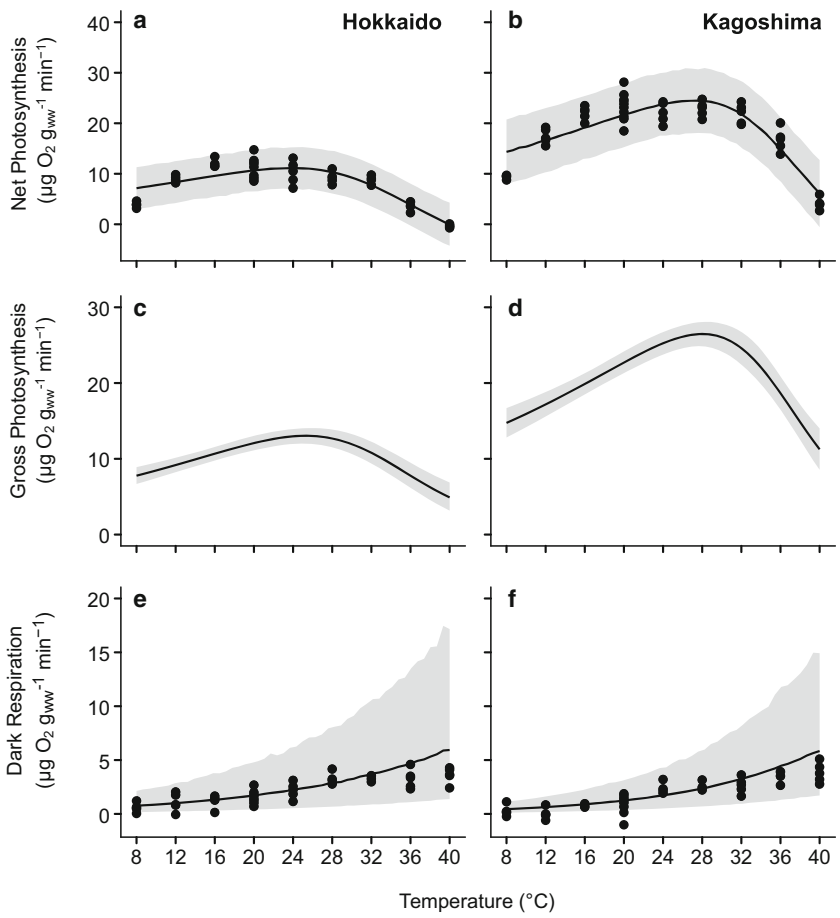

Fig. 2 The response of the oxygenic photosynthesis and dark respiration of a red alga, *Agarophyton vermiculophyllum* from the native range of distribution in Hokkaido (A, C, E) and Kagoshima (B, D, F), Japan to temperature (8, 12, 16, 20, 24, 28, 30, 32, 36, and 40°C; $n = 5$ at level). A, B: The response of net photosynthesis to temperature determined at 200 μmol photons m^{-2} s^{-1}. C, D: The modeled gross photosynthetic rates at 200 μmol photons m^{-2} s^{-1}. The data was derived from the model curve of net photosynthesis (A, B) and dark respiration (E, F). E, F: The response of dark respiration to temperature at 0 μmol photons m^{-2} s^{-1}. See the caption in Fig. 1 for the details

initial value; 0.291 ± 0.125 at 1-h, 60.6%; 0.064 ± 0.100 at 2-h, 13.4%; $P < 0.001$) and dropped to almost zero at 4-h and 8-h exposures, respectively (Fig. 4 B). In contrast, the $\Delta F/F_m'$ of alga at 30-min desiccation treatments returned to initial levels (0.468 ± 0.046, 100.8%) after subsequent 30-min rehydration in seawater (Fig. 4 D). Furthermore, those at 1-h desiccation treatment also returned to initial levels (0.472 ± 0.042, 101.4%) at subsequent 1-day rehydration (Fig. 4 F). However, those at 2-, 4-, and 8-h desiccation treatments failed to recover even after 1-day rehydration in seawater (0.245 ± 0.201 at 2-h, 52.6%; 0.009 ± 0.014 at 4-h, 1.9%; 0.004 ± 0.009 at 8-h, 0.9%; $P < 0.001$).

The fluctuation of the $\Delta F/F_m'$ of the alga was closely related to the decrease in the absolute water content (AWC) of the thallus under the desiccation (Fig. 5). For the Hokkaido strain, the $\Delta F/F_m'$ during the aerial desiccation state was generally stable between 0.451 ± 0.030 SD and 0.437 ± 0.020 when the AWC was 89.6% through 70.6%. However, it gradually decreased with decreasing AWC below 60.0%, and dropped to almost zero at AWC of less than 10% (Fig. 5 A). Nevertheless, for those under subsequent 30-min and 1-day rehydration in seawater treatments, the $\Delta F/F_m'$ almost recovered to initial levels at AWC above 40% (e.g., 0.458 ± 0.038, at AWC of 44.9%) at 30-min rehydration and 10% (e.g., 0.446 ± 0.032, at AWC of 14.1%); however, for AWC of less than 10%, $\Delta F/F_m'$ did not recover even after 1-d rehydration in seawater (Fig. 5 C, E).

The $\Delta F/F_m'$ of the alga from Kagoshima under the aerial desiccation state was also generally stable as between 0.457 ± 0.050 SD and 0.446 ± 0.052 when AWC was 88.1% through 85.1% (Fig. 5 B). However, it gradually decreased with decreasing AWC below 60.0%, and dropped to almost zero at an AWC of less than 10%. Nevertheless, for those under subsequent 30-min and 1-day rehydration in seawater treatments, the $\Delta F/F_m'$ almost recovered to the initial level at the AWC of above 40% (e.g., 0.425 ± 0.051, at AWC of 40.1%) at 30-min rehydration and 10% (e.g., 0.438 ± 0.072, at AWC of 11.4%); however, $\Delta F/F_m'$ for when AWC was less than 10% did not recover even after 1-day rehydration in seawater (Fig. 5 D, F).

The chronic effect of salinity gradient on the photochemical efficiency

The $\Delta F/F_m'$ of the algae from Hokkaido and Kagoshima at 3-day exposure under the salinity gradient was stable throughout the salinity treatments (Fig. 6 A, B). The $\Delta F/F_m'$ of the alga from Hokkaido at 7-day exposure was also stable at a salinity between 20 and 40 psu (0.516 ± 0.018 SD, 0.514 ± 0.016,

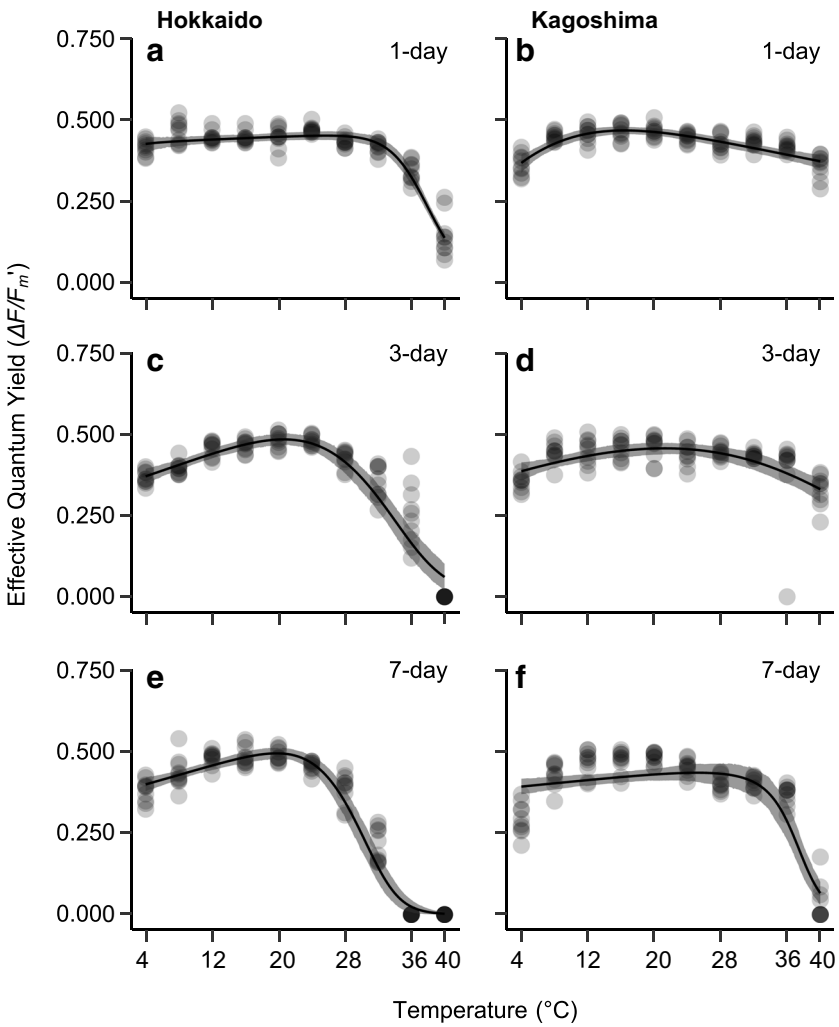

Fig. 3 The response of photochemical efficiency ($\Delta F/F_m'$) of the photosystem II in a red alga, *Agarophyton vermiculophyllum* from the native range of distribution in Hokkaido (A, C, E) and Kagoshima (B, D, F), Japan to temperature (4, 8, 12, 16, 20, 24, 28, 30, 32, 36, and 40°C) after 1 (A, B), 3 (C, D), and 7 days (E, F) under 50 μmol photons m^{-2} s^{-1} (14L10D photoperiod). The dots indicate the actual measured values (n = 10 at level), the lines indicate the expected value, and the shaded regions indicate the 95% highest density credible intervals (95% HDCI) of the model. Note that the varying shades of gray are due to overlaps of the dots, and do not indicate different treatments

0.497 ± 0.011, and 0.481 ± 0.018 at 20, 30, 34, and 40 psu); however, it decreased at 10 and 0 psu (0.293 ± 0.116 at 10 psu; 0.000 ± 0.000 at 0 psu; $P < 0.001$; Fig. 6 C). The $\Delta F/F_m'$ also slightly decreased at 50 and 60 psu (0.452 ± 0.014 and 0.451 ± 0.018 at 50 and 60 psu) but was not significantly different from 34 psu.

The $\Delta F/F_m'$ of the alga from Kagoshima at 7-day exposure was also stable at a salinity between 10 and 50 psu (0.460 ± 0.061 SD, 0.503 ± 0.034, 0.472 ± 0.041, 0.496 ± 0.016, 0.491 ± 0.034, 0.472 ± 0.042 at 10, 20, 30, 34, and 50 psu); however, it decreased at 0 psu (0.202 ± 0.144, $P < 0.001$; Fig. 6 D). The $\Delta F/F_m'$

Table 4 Mean and 95% highest density credible intervals (95% HDCI) of the parameters estimated for the photochemical efficiency of the photosystem II ($\Delta F/F_m'$)—temperature model in a red alga, *Agarophyton vermiculophyllum* from Hokkaido, Japan, exposed for 7-day temperature exposure between 4 and 40°C. $\Delta F/F_m'$ = effective quantum yield; H_a = activation energy for photosynthesis (kJ mol^{-1}); H_d = deactivation energy (kJ mol^{-1}); $T_{opt}^{\Delta F/Fm'}$ = optimum temperature (°C)

	1-day		3-day		7-day	
Parameter	Mean	95% HDCI	Mean	95% HDCI	Mean	95% HDCI
$\Delta F/F_m'_{(max)}$	0.45	0.44–0.46	0.49	0.47–0.50	0.50	0.48–0.51
H_a	2	1–3	16	10–23	12	7–17
H_d	350	291–410	144	108–182	221	163–282
$T_{opt}^{\Delta F/Fm'}$	26.1	24.2–28.0	21.0	19.3–22.6	20.0	18.5–21.5

Table 5 Mean and 95% highest density credible intervals (95% HDCI) of the parameters estimated for the photochemical efficiency of the photosystem II ($\Delta F/F_m'$)—temperature model in a red alga, *Agarophyton vermiculophyllum* from Kagoshima, Japan, exposed for 7-day temperature exposure between 4 and 40°C. $\Delta F/F_m'$ = effective quantum yield; H_a = activation energy for photosynthesis (kJ mol^{-1}); H_d = deactivation energy (kJ mol^{-1}); $T_{opt}^{\Delta F/Fm'}$ = optimum temperature (°C)

	1-day		3-day		7-day	
Parameter	Mean	95% HDCI	Mean	95% HDCI	Mean	95% HDCI
$\Delta F/F_m'$ $_{(max)}$	0.47	0.46–0.48	0.46	0.45–0.48	0.46	0.43–0.48
H_a	84	33–137	17	2–41	4	2–6
H_d	96	53–141	90	49–169	503	336–686
$T_{opt}^{\Delta F/Fm'}$	16.5	14.1–18.9	22.3	17.4–26.9	30.1	27.9–32.2

was also slightly decreased at 60 psu (0.414 ± 0.065)but was not significantly different from 34 psu.

Discussion

In Japan *A. vermiculophyllum* generally occurs on rocks and pebbles in the lower intertidal zone of sheltered bays, inlets, estuaries, and salt marshes (Terada et al. 2000, 2010; Terada and Yamamoto 2002). The annual range of mean seawater temperatures in the two locations is different, ranging from 4 to 24°C in Hokkaido (Hakodate) and from 14 to 28°C in Kagoshima (Terada et al. 2000, 2021; Watanabe et al. 2014).

In the present study, the response of oxygenic photosynthesis and photochemical efficiency of the PSII in the Hokkaido (north) and Kagoshima (south) strains generally showed similar responses to temperature, irradiance, desiccation, and salinity. In fact, oxygenic *P–E* curves of each strain

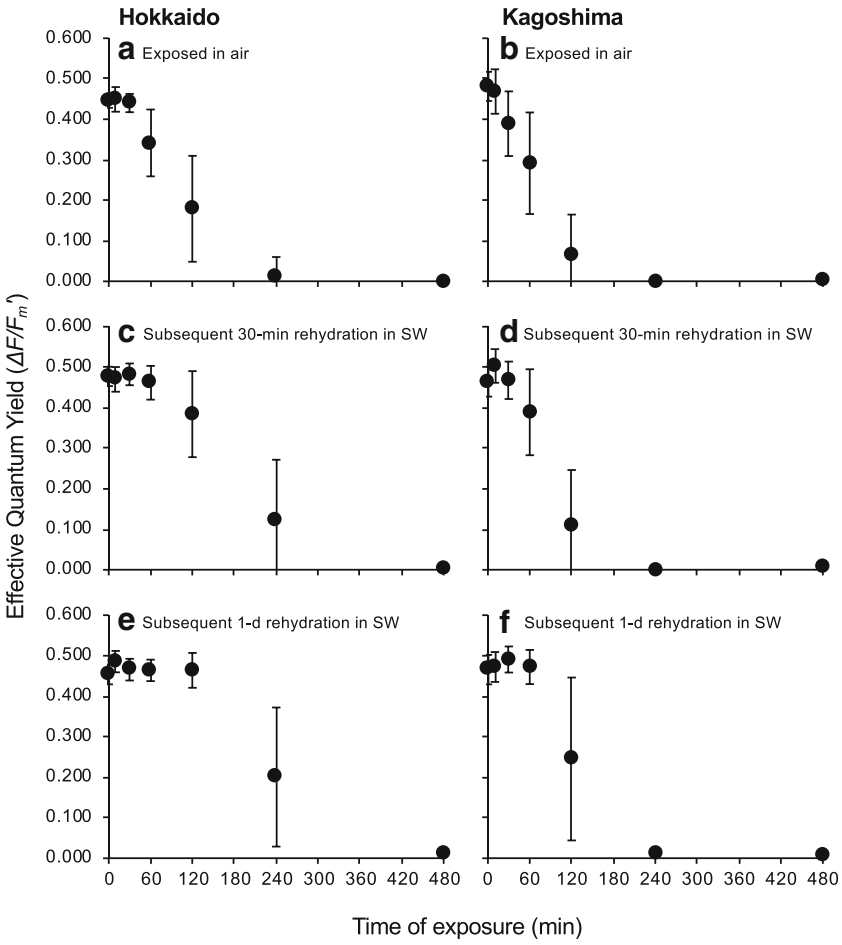

Fig. 4 The chronological response of photochemical efficiency ($\Delta F/F_m'$) of the photosystem II in a red alga, *Agarophyton vermiculophyllum* from the native range of distribution in Hokkaido (A, C, E) and Kagoshima (B, D, F), Japan to aerial exposure at the humidity of 50% under the dim-light (20 μmol photons m^{-2} s^{-1}). The symbols indicate the average of actual values measured (n = 50), and bars indicate standard deviation. Six figures indicate measurements exposed in air (A, B), those in subsequent 30-min (C, D) and 1-day rehydration (E, F) in seawater, respectively

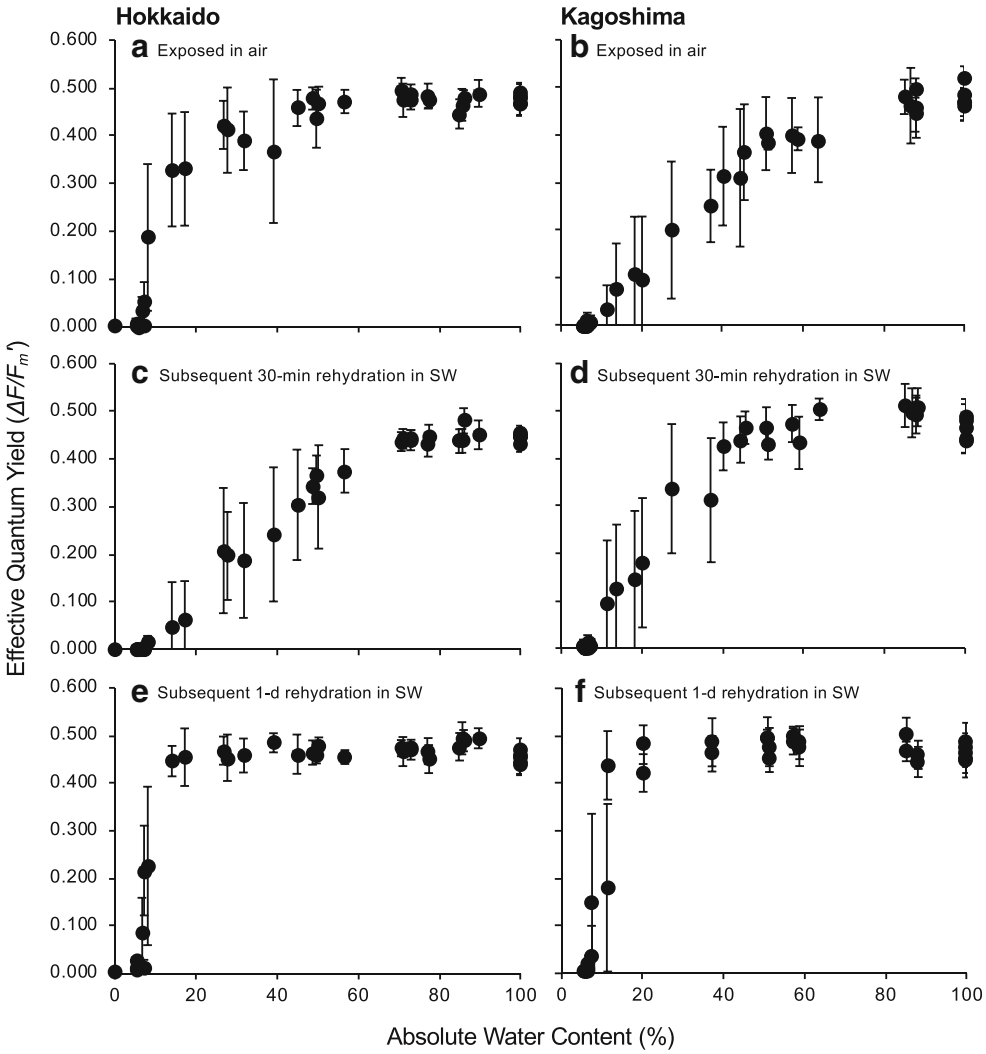

Fig. 5 The relationship between photochemical efficiency ($\Delta F/F_m'$) of the photosystem II and the absolute water content (AWC, %) in a red alga, *Agarophyton vermiculophyllum* from the native range of distribution in Hokkaido (A, C, E) and Kagoshima (B, D, F) Japan to aerial exposure at the humidity of 50% under the dim light (20 μmol photons m^{-2} s^{-1}). The symbols indicate the average of actual values measured (n = 10), and bars indicate standard deviation. Six figures indicate measurements exposed in air (A, B), those in subsequent 30-min (C, D) and 1-day rehydration (E, F) in seawater, respectively

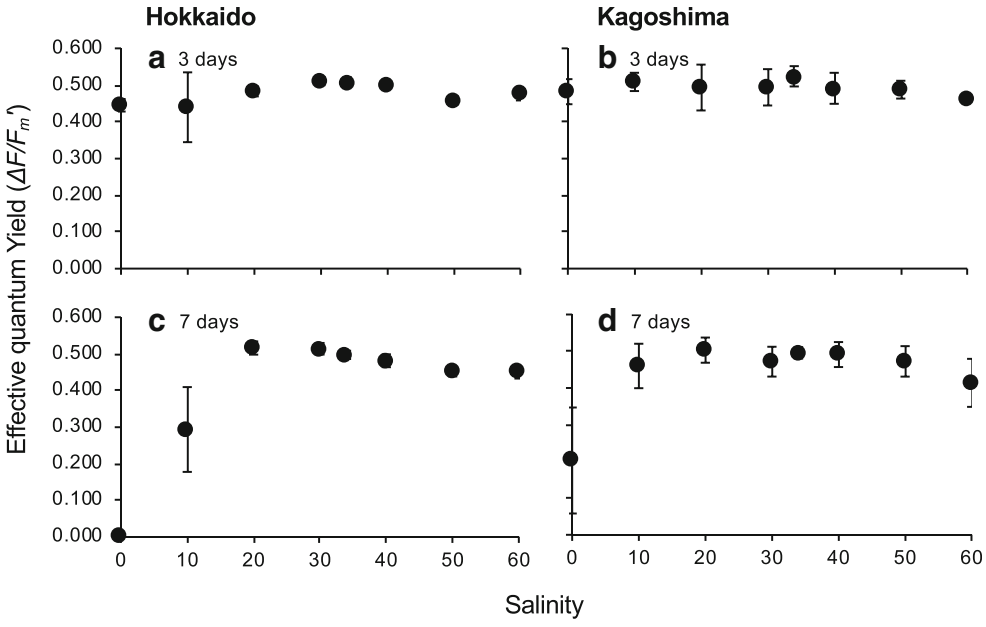

Fig. 6 The response of photochemical efficiency ($\Delta F/F_m'$) of the photosystem II in a red alga, *Agarophyton vermiculophyllum* from Hokkaido (A, C) and Kagoshima (B, D) at eight salinity treatments (0, 10, 20, 30, 34, 40, 50, and 60 psu) after 3 (A, B) and 7 (C, D) days under the dim-light (20 μmol photons m^{-2} s^{-1}). The dots indicate the measured values (n = 10), and bars indicate standard deviation

at 8, 16, 28°C were temperature-dependent, and the maximum net photosynthesis (NP_{max}) was highest at 28°C, and was lowest at 8°C; these results corresponded well with the measured *NP* and estimated *GP* rates in the *P–T* response experiment. Furthermore, saturation-irradiances (E_k) were also temperature-dependent with the highest value at 28°C (423 and 499 μmol photons m^{-2} s^{-1} for Hokkaido and Kagoshima, respectively), signifying that the light requirement to reach photosynthetic saturation gradually increases with increasing temperature. In fact, given that the initial slopes (α) of the *P–E* curve were generally similar, except for the samples at 8°C from Kagoshima, the relatively high values of NP_{max} at high temperature is believed to be due to the increase of E_k as temperature increased. In contrast, at 8°C, the NP_{max} was strongly suppressed as it was quickly saturated at low irradiances, and this result corresponds well with those of the oxygenic *P–T* responses. Hence, strong light might not be needed to saturate the photosynthesis in winter due to the low value of NP_{max}.

The strains of Hokkaido (north) and Kagoshima (south) showed similar responses in the *P–E* curves at 8, 16, and 28°C; nevertheless, the values of NP_{max} were higher in Kagoshima than those of Hokkaido except for those at 8°C. Given that the distributions of two haplotypes are roughly separated latitudinally in the northern and southern part of Japan, it might be a result of adaptation to each abiotic environment in two haplotypes (Krueger-Hadfield et al. 2017). In fact, maximum gross photosynthesis (GP_{max}) in the *GP–T* responses in Hokkaido and Kagoshima was 13.09 (12.05–14.10, 95% HDCI) and 26.56 (24.96–28.19, 95% HDCI) μg O_2 g_{ww}^{-1} min^{-1}, and was occurred at 25.3 (23.2–27.6, 95% HDCI) and 28.0°C (26.0–29.9, 95% HDCI), respectively (T_{opt}^{GP}), which are near the highest summertime seawater temperature at two locations, indicating that GP_{max} and T_{opt}^{GP} were also higher in Kagoshima (south) than those of Hokkaido (north).

Likewise, the $\Delta F/F_m'$ of PSII response in 7-day cultivation over a range of temperatures (4–40°C) also showed a single peak with the highest vales ($\Delta F/F_m'_{max}$) at 20.0°C (18.5–21.5, 95% HDCI) for Hokkaido and 30.1°C (27.9–32.2, 95% HDCI; $T_{opt}^{\Delta F/Fm'}$) for Kagoshima, respectively. However, the responses under the thermal stress above the optimal temperature were different in two locations. In fact, the $\Delta F/F_m'$ from Hokkaido strain gradually decreased above the optimal temperature and suddenly dropped to zero at 36°C. Those of Kagoshima also decreased above the optimal temperature but was well tolerated except for those at 40°C. The $\Delta F/F_m'$ of PSII and oxygenic photosynthesis (*GP* rates) of the two strains over the same temperature range also showed a similar decline above optimal temperature. Given the decline in $\Delta F/F_m'$ of PSII and oxygenic *GP* rates above 36°C, heat stress may be occurring, and hence PSII deactivation, since thermal stress is related to structural rearrangement in the thylakoid membranes (Roleda 2009) or to an accumulation of hydrogen peroxide that inhibits *de novo* synthesis of D_1 protein in PSII (Allakhverdiev and Murata 2004; Allakhverdiev et al. 2008; Takahashi and Murata 2008). Also, relatively long temperature exposure (i.e., 7-d exposure) may also negatively influence all metabolic processes in the thalli especially at high temperatures, and enhance the decline of the photochemical efficiency of the alga.

Likewise, given the decline in $\Delta F/F_m'$ of PSII and oxygenic *GP* and *NP* rates below 8°C, the low temperature also suppressed the photosynthetic activities of this alga and it seemed to be more pronounced in the Kagoshima strain. In fact, low temperature is known to inhibit the fixation of carbon dioxide with a resultant generation of reactive oxygen species (ROS), which in turn suppressed the de novo synthesis of the D_1 protein, further reducing the repair of PSII and resulting in more severe damage to PSII (Allakhverdiev and Murata 2004). Consequently, given that the strains from Hokkaido and Kagoshima were in the different temperature environments, this alga from two locations can be regarded to be well adapted to relatively low and warm temperatures, respectively, in relation to their respective habitats.

In general, *A. vermiculophyllum* populations in Japan inhabit the lower intertidal zone which experience periodic immersion and emersion (Terada et al. 2000, 2010). As revealed in the desiccation experiment, the $\Delta F/F_m'$ of PSII in each strain under the dehydrated state decreased with increasing aerial exposure period. However, despite the decrease of $\Delta F/F_m'$ of the PSII under dehydrated state, the values within 2-h desiccation state for the Hokkaido strain and 1-h desiccation state for the Kagoshima strain generally recovered to initial levels after a subsequent 1-day rehydration in seawater, showing the strong ability to recover from aerial exposure. The difference of tolerable duration under desiccation state in the two strains was considered to be due to the difference in thickness of the thallus in relation to water loss, as the samples from Hokkaido were thicker and almost twice that of samples from Kagoshima (1.35 mm ± 0.19 SD and 0.76 mm ± 0.13 SD, respectively). Nevertheless, $\Delta F/F_m'$ values dropped to almost zero at more than 4-h air exposures under a humidity of 50%, with the absence of complete recovery after subsequent rehydration in seawater. Indeed, critical water loss was observed in samples under these desiccation treatments, with less than 60% AWC leading to reductions in $\Delta F/F_m'$ under a desiccation state.

Photosynthetic activity is known to be negatively correlated with loss of water content in the cell (Dring and Brown 1982; Ji and Tanaka 2002; Contreras-Porcia et al. 2011; Hurd et al. 2014). Cellular dehydration resulting from desiccation increases electrolyte concentration in the cell, and brings changes to membrane structures including thylakoids (Wiltens et al. 1978; Kim and Garbary 2007), which result in a decline in photosynthetic rate while interrupting the

electron flow between photosystem I (PSI) and PSII (Gao et al. 2011). Likewise, the poor photosynthetic performance in desiccated algae is also reported to be associated with multiple cellular changes and loss of volume that resulted in a dysfunction, including loss of its repair capacity (e.g., *Caulerpa lentillifera*; Flores-Molina et al. 2014; Terada et al. 2018). Nevertheless, in the present study, the $\Delta F/F_m'$ of PSII under a desiccated state with AWC above 20% were restored to initial levels following 1-day rehydration in seawater, suggesting potential of photosynthetic recovery of this alga at such a low hydration threshold (Davison and Peason 1996; Holzinger and Karsten 2013; Beer et al. 2014). In fact, in an intertidal red alga *Pyropia columbina* (Montagne) Nelson, overproduction of ROS with the inhibition of antioxidant enzymes is reported to be observed during the desiccation, but this was efficiently attenuated after rehydration in seawater (Contreras-Porcia et al. 2011).

Under the extreme hypo- or hypersaline stresses, algal cells are thought to increase ionic concentrations but also to undergo a change in ion ratios due to selective uptake; therefore, photosynthesis and respiration are also known to be inhibited in marine algae under these stresses (Kirst 1989). In fact, the initial charge separations at the reaction centers of PSI and PSII are thought to be inhibited by ionic stress. In addition, osmotic stress is assumed to increase the permeability of the thylakoids to ions (e.g., Na^+, Cl^-, K^+), which subsequently inhibit PSI and PSII (Kirst 1989).

In the present study, the photochemical efficiency of *A. vermiculophyllum* from the Hokkaido and Kagoshima strains seemed to be stable to a broad range of salinity (20–60 psu) as observed from the 7-day culture, except for salinities below 10 psu. These results corresponded well with previous studies regarding growth response to salinity (Yokoya et al. 1999; Raikar et al. 2001; Rueness 2005; Thomsen et al. 2007; Nejrup and Pedersen 2012), suggesting that this alga from both native and non-native ranges are well adapted to a euryhaline environment. In fact, given that this alga can often be found in estuarine areas, influenced by freshwater input from rivers, the $\Delta F/F_m'$ of PSII tolerated 0 psu at 3-day exposure; therefore, this alga seems to have a tolerance to hyposaline conditions, which can be observed in other estuarine species (e.g., *Enteromorpha*, Martins et al. 1999; Dan et al. 2002). Nevertheless, as the $\Delta F/F_m'$ of PSII dropped at 0 psu after 7-day exposure, the ability to tolerate low salinities may only last for a short duration; however, our observations suggest that *A. vermiculophyllum* is more than able to flourish in estuarine areas.

In conclusion, the tolerance of *A. vermiculophyllum* collected from its native range in Japan to relatively high irradiance, broad range of temperatures, and osmotic stress (desiccation and salinity) may explain its potentially high invasive capacity. However, as we monitored only the responses of photosynthesis under environmental gradients, the mechanisms of such tolerance in this alga have not been yet elucidated. More interestingly, recent studies suggest that rapid phenotypic evolution occurs during invasion that enables adaptation to non-native regions (Krueger-Hadfield et al. 2016, 2017; Sotka et al. 2018). Therefore, further studies of the photosynthetic responses to environmental gradients are required including the alga that is in the non-native range.

Acknowledgements We thank colleague and lab mates, Hikaru Endo, Iris Ann Borlongan (present: University of the Philippines Visayas), Jumpei Kozono (present: Japan Wildlife Research Center) for their kind assistance in the present study. All authors have provided consent.

Funding This research was supported in part by the Grant-in-Aid for Scientific Research (B; #16H02939, #20H03076) from Japan Society for the Promotion of Science (JSPS).

Data availability The datasets generated in the present study are available from the corresponding author on reasonable request.

References

Alexandrov GA, Yamagata Y (2007) A peaked function for modeling temperature dependence of plant productivity. Ecol Model 200: 189–192

Allakhverdiev SI, Kreslavski VD, Klimov VV, Los DA, Carpentier R, Mohanty P (2008) Heat stress: an overview of molecular responses in photosynthesis. Photosynth Res 98:541–550

Allakhverdiev SI, Murata N (2004) Environmental stress inhibits the synthesis de novo of proteins involved in the photodamage-repair cycle of photosystem II in *Synechocystis* sp. PCC 6803. Biochim Biophys Acta 1657:23–32

Barrett EM (1963) The California oyster industry. Fish Bull 123:1–53

Beer S, Biörk M, Beardall J (2014) Photosynthesis in the marine environment. Wiley-Blackwell, Ames, Iowa

Bellasio C, Burgess SJ, Griffiths H, Hibberd JM (2014) A high throughput gas exchange screen for determining rates of photorespiration or regulation of C4 activity. J Exp Bot 65:3769–3779

Bellorin AM, Oliveira MC, Oliveira EC (2004) *Gracilaria vermiculophylla*: A western Pacific species of Gracilariaceae (Rhodophyta) first recorded from the eastern Pacific. Phycol Res 52:69–79

Boo SM, Ko YD (2012) Marine plants from Korea. Marine and Extreme Genome Research Centre Program, Seoul (in Korean)

Borlongan IA, Arita R, Nishihara GN, Terada R (2020) The effects of temperature and irradiance on the photosynthesis of two heteromorphic life history stages of *Saccharina japonica* (Laminariales) from Japan. J Appl Phycol 32:4175–4187

Bürkner PC (2018) Advanced Bayesian multilevel modeling with the R Package brms. R J 10:395–411

Byers JE, Gribben PE, Yeager C, Sotka EE (2012) Impacts of an abundant introduced ecosystem engineer within mudflats of the southeastern US coast. Biol Invasions 149:2587–2600

Contreras-Porcia L, Thomas D, Flores V, Correa JA (2011) Tolerance to oxidative stress induced by desiccation in *Porphyra columbina* (Bangiales, Rhodophyta). J Exp Bot 62:1815–1829

Dan A, Hiraoka M, Ohno M, Critcheley AT (2002) Observations on the effect of salinity and photon fluence rate on the induction of sporulation and rhizoid formation in the green alga *Enteromorpha prolifera* (Müller) J. Agardh (Chlorophyta, Ulvales). Fish Sci 68: 1182–1188

Davison IR, Peason GA (1996) Stress tolerance in intertidal seaweeds. J Phycol 32:197–211

Dring MJ, Brown FA (1982) Photosynthesis of intertidal brown algae during and after periods of emersion: a renewed search for physiological causes of zonation. Mar Ecol Prog Ser 8:301–308

Flores-Molina MR, Thomas D, Lovazzanoc C, Núñez A, Zapata J, Kumar M, Correa JA, Contreras-Porcia L (2014) Desiccation stress in intertidal seaweeds: Effects on morphology, antioxidant responses and photosynthetic performance. Aquat Bot 113:90–99

Freshwater DW, Greene JK, Hamner RM (2006a) Seasonality of the invasive seaweed *Gracilaria vermiculophylla* along the southeastern coast of North Carolina. J North Carolina Acad Sci 122:49–55

Freshwater DW, Montgomery F, Greene JK, Hammer RM, Williams M, Whitfield PE (2006b) Distribution and identification of an invasive *Gracilaria* species that is hampering commercial fishing operations in southeastern North Carolina, USA. Biol Invasions 8:631–637

Gao S, Niu J, Chen W, Wang G, Xie X, Pan G, Gu W, Zhu D (2013) The physiological links of the increased photosystem II activity in moderately desiccated *Porphyra haitanensis* (Bangiales, Rhodophyta) to the cyclic electron flow during desiccation and re-hydration. Photosynth Res 116:45–54

Gao S, Shen S, Wang G, Niu J, Lin A, Pan G (2011) PSI-driven cyclic electron flow allows intertidal macro-algae *Ulva* sp. (Chlorophyta) to survive in desiccated conditions. Plant Cell Physiol 52:885–893

Gao S, Wang G (2012) The enhancement of cyclic electron flow around photosystem I improves the recovery of severely desiccated *Porphyra yezoensis* (Bangiales, Rhodophyta). J Exp Bot 63:4349–4358

Gelman A (2004) Parameterization and Bayesian Modeling. J Am Stat Assoc 99:537–545

Gelman A (2006) Prior distributions for variance parameters in hierarchical models. Bayesian Anal 1:515–533

Gorman L, Kraemer GP, Yarish C, Boo SM, Kim JK (2017) The effects of temperature on the growth rate and nitrogen content of invasive *Gracilaria vermiculophylla* and native *Gracilaria tikvahiae* from Long Island Sound, USA. Algae 32:57–66

Gurgel CFD, Norris JN, Schmidt WE, Le HN, Fredericq S (2018) Systematics of the Gracilariales (Rhodophyta) including new subfamilies, tribes, subgenera, and two new genera, *Agarophyton gen. nov*. and *Crassa gen. nov*. Phytotaxa 374:1–23

Hammann M, Buchholz B, Karez R, Weinberger F (2013a) Direct and indirect effects of *Gracilaria vermiculophylla* on native *Fucus vesiculosus*. Aquat Invasions 8:121–132

Hammann M, Wang G, Rickert E, Boo SM, Weinberger F (2013b) Invasion success of the seaweed *Gracilaria vermiculophylla* correlates with low palatability. Mar Ecol Prog Ser 486:93–103

Henley WJ (1993) Measurement and interpretation of photosynthetic light-response curves in algae in the context of photo inhibition and diel changes. J Phycol 29:729–739

Holzinger A, Karsten U (2013) Desiccation stress and tolerance in green algae: consequences for ultrastructure, physiological, and molecular mechanisms. Front Plant Sci 4:327

Hurd CL, Harrison PJ, Bischof K, Lobban CS (2014) Seaweed ecology and physiology, 2nd edn. Cambridge University Press, Cambridge

Jassby AD, Platt T (1976) Mathematical formulation of the relationship between photosynthesis and light for phytoplankton. Limnol Oceanogr 21:540–547

Ji Y, Tanaka J (2002) Effect of desiccation on the photosynthesis of seaweeds from the intertidal zone in Honshu, Japan. Phycol Res 50:145–153

Kim KY, Garbary DJ (2007) Photosynthesis in *Codium fragile* (Chlorophyta) from a Nova Scotia estuary: responses to desiccation and hyposalinity. Mar Biol 151:99–107

Kim SY, Weinberger F, Boo SM (2010) Genetic data hint at a common donor region for invasive Atlantic and Pacific populations of *Gracilaria vermiculophylla* (Gracilariales, Rhodophyta). J Phycol 46:1346–1349

Kirst GO (1989) Salinity tolerance of eukaryotic marine algae. Annu Rev Plant Physiol Plant Mol Biol 41:21–53

Kokubu S, Nishihara GN, Watanabe Y, Tsuchiya Y, Amano Y, Terada R (2015) The effect of irradiance and temperature on the photosynthesis of a native brown alga, *Sargassum fusiforme* (Fucales) from Kagoshima, Japan. Phycologia 54:235–247

Krueger-Hadfield SA, Kollars NM, Byers JE, Greig TW, Hammann M, Murray DC, Murren CJ, Strand AE, Terada R, Weinberger F, Sotka EE (2016) Invasion of novel habitats uncouples haplo-diplontic life cycles. Mol Ecol 25:3801–3816

Krueger-Hadfield SA, Kollars NM, Strand AE, Byers JE, Shainker SJ, Terada R, Greig TW, Hammann M, Murray DC, Weinberger F, Sotka EE (2017) Genetic identification of source and likely vector of a widespread marine invader. Ecol Evol 7:4432–4447

Maggi E, Benedetti-Cecchi L, Castelli A, Chatzinikolaou E, Crowe TP, Ghedini G, Kotta J, Lyons DA, Ravaglioli C, Rilov G, Rindi L, Bulleri F (2015) Ecological impacts of invading seaweeds: a meta-analysis of their effects at different trophic levels. Divers Distrib 21:1–12

Martínez-Lüscher J, Holmer M (2010) Potential effects of the invasive species *Gracilaria vermiculophylla* on *Zostera marina* metabolism and survival. Mar Environ Res 69:345–349

Martins I, Oliveira JM, Flindt MR, Marques JC (1999) The effect of salinity on the growth rate of the macroalgae *Enteromorpha intestinalis* (Chlorophyta) in the Mondego estuary (west Portugal). Acta Oecol 20:259–265

Nejrup LB, Pedersen MF (2012) The effect of temporal variability in salinity on the invasive red alga *Gracilaria vermiculophylla*. Eur J Phycol 47:254–263

Nejrup LB, Staehr PA, Thomsen MS (2013) Temperature- and light-dependent growth and metabolism of the invasive red algae *Gracilaria vermiculophylla* – a comparison with two native macroalgae. Eur J Phycol 48:295–308

Ohmi H (1956) Contributions to the knowledge of Gracilariaceae from Japan. II. On a new species of the genus *Gracilariopsis* with some considerations on its ecology. Bull Fac Fish Hokaido Univ 6:271–279

Ohmi H (1958) The species of *Gracilaria* and *Gracilariopsis* from Japan and adjacent waters. Mem Fac Fish Hokkaido Univ 6:1–66

Ohno M, Largo DB (1998) The seaweed resources of Japan. In: Critchley AT, Ohno M (eds) Seaweed resources of the world. Japan International Cooperation Agency, Kanagawa, pp 1–14

Phooprong S, Ogawa H, Hayashizaki K (2008) Photosynthetic and respiratory responses of *Gracilaria vermiculophylla* (Ohmi) Papenfuss collected from Kumamoto, Shizuoka and Iwate, Japan. J Appl Phycol 20:743–750

Platt T, Gallegos CL, Harrison WG (1980) Photoinhibition of photosynthesis in natural assemblages of marine phytoplankton. J Mar Res 38:687–701

R Development Core Team (2020) R: A language and environment for statistical computing. R Foundation for Statistical Computing, Vienna. http://www.R-project.org (acessed on 10 December 2020)

Raikar SV, Iima M, Fujita Y (2001) Effect of temperature, salinity and light intensity on the growth of *Gracilaria* spp. (Gracilariales, Rhodophyta) from Japan, Malaysia and India. Indian J Mar Sci 30:98–104

Roleda MY (2009) Photosynthetic response of Arctic kelp zoospores exposed to radiation and thermal stress. Photochem Photobiol Sci 9:1302–1312

Ruesink JL, Lenihan HS, Trimble AC, Heiman KW, Micheli F, Byers JE, Kay MC (2005) Introduction of non-native oysters: ecosystem effects and restoration implications. Annu Rev Ecol Evol Syst 36:643–689

Rueness J (2005) Life history and molecular sequences of *Gracilaria vermiculophylla* (Gracilariales, Rhodophyta), a new introduction to European waters. Phycologia 44:120–128

Saunders GW (2009) Routine DNA barcoding of Canadian Gracilariales (Rhodophyta) reveals the invasive species *Gracilaria vermiculophylla* in British Columbia. Mol Ecol Resour 9:140–150

Sotka EE, Baumgardner AW, Bippus PM, Destombe C, Duermit EA, Endo H, Flanagan BA, Kamiya M, Lees LE, Murren CJ, Nakaoka M, Shainker SJ, Strand AE, Terada R, Valero M, Weinberger F, Krueger-Hadfield SA (2018) Combining niche shift and population genetic analyses predicts rapid phenotypic evolution during invasion. Evol Appl 11:781–793

Stan Development Team (2020) Stan: A C++ Library for Probability and Sampling, Version 2.18.9. http://mc-stan.org (Acessed on 10 April 2020)

Takahashi S, Murata N (2008) How do environmental stresses accelerate photoinhibition? Trends Plant Sci 13:178–182

Tcherkez G, Bligny R, Gout E, Mahé A, Hodges M, Cornic G (2008) Respiratory metabolism of illuminated leaves depends on CO_2 and O_2 conditions. Proc Natl Acad Sci U S A 105:797–802

Terada R, Abe M, Abe T, Aoki M, Dazai A, Endo H, Kamiya M, Kawai H, Kurashima A, Motomura T, Murase N, Sakanishi Y, Shimabukuro H (2021) Japan's nationwide long-term monitoring survey of seaweed communities known as the "*Monitoring Sites 1000*": Ten-year overview and future perspectives. Phycol Res 69: 12–30

Terada R, Abe T, Kawaguchi S (2010) Reproductive phenology of three species of *Gracilaria*: *G. blodgettii* Harvey, *G. vermiculophylla* (Ohmi) Papenfuss and *G. salicornia* (C. Agardh) Dawson (Gracilariales, Rhodophyta) from Okinawa, Ryukyu Islands, Japan. Coast Mar Sci 34:129–134

Terada R, Kimura M, Yamamoto H (2000) Growth and maturation of *Gracilaria vermiculophylla* (Ohmi) Papenfuss from Hakodate, Hokkaido, Japan. Jpn J Phycol 48:203–209 (in Japanese with English abstract)

Terada R, Nakashima Y, Borlongan IA, Shimabukuro H, Kozono J, Endo H, Shimada S, Nishihara GN (2020a) Photosynthetic activity including the thermal- and chilling-light sensitivities of a temperate Japanese brown alga *Sargassum macrocarpum*. Phycol Res 68: 70–79

Terada R, Nakazaki Y, Borlongan IA, Endo H, Nishihara GN (2018) Desiccation effect on the PSII photochemical efficiency of cultivated Japanese *Caulerpa lentillifera* under the shipping package environment. J Appl Phycol 30:2533–2588

Terada R, Yamamoto H (2002) Review of *Gracilaria vermiculophylla* (Ohmi) Papenfuss and other species in Japan and Asia. In: Abbott IA, McDermid K (eds) Taxonomy of economic seaweeds, with special reference to Pacific species Volume 8. California Sea Grant College Program, University of California, La Jolla, pp 225–230

Terada R, Yuge T, Watanabe Y, Mine T, Morikawa T, Nishihara GN (2020b) Chronic effects of three different stressors, irradiance, temperature, and desiccation on the PSII photochemical efficiency in the heteromorphic life-history stages of cultivated *Pyropia yezoensis* f. *narawaensis* (Bangiales) from Japan. J Appl Phycol 32:3273–3284

Titlyanov EA, Titlyanova TV (2012) Marine plants of the Asian Pacific region countries, their use and cultivation. A.V. Zhirmunsky Institute of Marine Biology Ear East Branch of the Russian Academy of Sciences, Dalnauka, Vladivostok

Thomsen MS, Gurgel CFD, Fredericq S, McGlathery KJ (2006) *Gracilaria vermiculophylla* (Rhodophyta, Gracilariales) in Hog Island Bay, Virginia: a cryptic alien and invasive macroalga and taxonomic correction. J Phycol 42:139–141

Thomsen MS, McGlathery KJ, Schwarzschild A, Silliman BR (2009) Distribution and ecological role of the non-native macroalga *Gracilaria vermiculophylla* in Virginia salt marshes. Biol Invasions 11:2303–2316

Thomsen MS, Staehr PA, Nyberg CD, Schwærter S, Krause-Jensen D, Silliman BR (2007) *Gracilaria vermiculophylla* (Ohmi) Papenfuss, 1967 (Rhodophyta, Gracilariaceae) in northern Europe, with emphasis on Danish conditions, and what to expect in the future. Aquat Invasions 2:83–94

Thornley JHM, Johnson IR (2000) Plant and Crop Modelling: A mathematical approach to plant and crop physiology. Blackburn Press, Caldwell, NJ

Tseng CK, Xia BM (1999) On the *Gracilaria* in the Western Pacific and the Southeastern Asia Region. Bot Mar 42:209–217

Wallentinus I, Nyberg CD (2007) Introduced marine organisms as habitat modifiers. Mar Pollut Bull 55:323–332

Wang WJ, Wang FJ, Zhu JY, Sun XT, Yao CY, Xu P (2011) Freezing tolerance of *Porphyra yezoensis* (Bangiales, Rhodophyta) gametophyte assessed by chlorophyll fluorescence. J Appl Phycol 23: 1017–1022

Watanabe Y, Nishihara GN, Tokunaga S, Terada R (2014) The effect of irradiance and temperature responses and the phenology of a native alga, *Undaria pinnatifida* (Laminariales), at the southern limit of its natural distribution in Japan. J Appl Phycol 26:2405–2415

Watanabe Y, Yamada H, Mine Y, Kawamura Y, Nishihara GN, Terada R (2017) Chronological change and the potential of recovery on the photosynthetic efficiency of *Pyropia yezoensis* f. *narawaensis* (Bangiales) during the sporelings frozen storage treatment in the Japanese Nori cultivation. Phycol Res 65:265–271

Webb WL, Newton M, Starr D (1974) Carbon dioxide exchange of *Alnus rubra*: a mathematical model. Oecologia 17:281–291

Weinberger F, Buchholz B, Karez R, Wahl M (2008) The invasive red alga *Gracilaria vermiculophylla* in the Baltic Sea: adaptation to brackish water may compensate for light limitation. Aquat Biol 3: 251–264

Wiltens J, Schreiber U, Vidaver W (1978) Chlorophyll fluorescence induction: an indicator of photosynthetic activity in marine algae understanding desiccation. Can J Bot 56:2787–2794

Williams SL, Smith J (2007) A global review of the distribution, taxonomy, and impacts of introduced seaweeds. Annu Rev Ecol Evol Syst 38:327–359

Yamamoto H (1978) Systematic and anatomical study of the genus *Gracilaria* in Japan. Mem Fac Fish Hokkaido Univ 25:97–152

Yokoya NS, Kakita H, Obika H, Kitamura T (1999) Effects of environmental factors and plant growth regulators on growth of the red alga *Gracilaria vermiculophylla* from Shikoku Island, Japan. Hydrobiologia 398:339–347